# Stray-field-induced quadrupole shift and absolute frequency of the 688-THz $^{171}Yb^+$ single-ion optical frequency standard

Chr. Tamm, S. Weyers, B. Lipphardt, and E. Peik
*Physikalisch-Technische Bundesanstalt, Bundesallee 100, 38116 Braunschweig, Germany*
(Received 7 July 2009; published 6 October 2009)

We report experimental investigations of a single-ion optical frequency standard based on $^{171}Yb^+$. The ion is confined in a cylindrically symmetric radiofrequency Paul trap. The reference transition is the $^2S_{1/2}(F=0)-^2D_{3/2}(F'=2)$ electric quadrupole transition at 688 THz. Using a differential measurement scheme, we determine the shift of the reference transition frequency that occurs due to the interaction of the electric quadrupole moment of the $^2D_{3/2}$ state with the gradient of the electrostatic stray field in the trap. We determine an upper limit for the instability of the quadrupole shift over times between 100 s to 20 h. We also observe the variations in the shift and in the applied stray-field compensation voltages that result from loading a new ion into the trap and during a subsequent storage period of 74 days. This information is utilized to measure the absolute frequency of the reference transition with an uncertainty that is a factor of 3 smaller than that of the previous measurement. Using a fiber laser based optical frequency comb generator and the cesium fountain clock CSF1 of PTB (Physikalisch-Technische Bundesanstalt), the frequency at 300 K temperature is determined as 688 358 979 309 306.62 ± 0.73 Hz.

DOI: 10.1103/PhysRevA.80.043403 PACS number(s): 37.10.Ty, 06.30.Ft, 32.10.Dk, 42.62.Eh

## I. INTRODUCTION

Optical frequency standards based on narrow-linewidth transitions in laser-cooled single ions or neutral atoms are currently being developed worldwide, and systematic uncertainties of $10^{-16}$ and below have been demonstrated [1,2]. This accuracy provides the foundation for a wide range of precision measurements and tests of fundamental physical theories and opens up the possibility of a primary time standard based on an optical clock. A number of different ion species are presently being investigated, including the ions $In^+$ [3] and $Al^+$ [2], which have an alkaline-earth-metal-like energy-level system, and the ions $Ca^+$ [4], $Sr^+$ [5,6], $Yb^+$ [7,8], and $Hg^+$ [9] whose level system is similar to that of alkali-metal atoms. The alkaline-earth-metal-like ions offer the advantage of a relatively low sensitivity of the transition frequency to electric fields and room-temperature blackbody radiation. Optical frequency standards based on alkali-metal-like ions are technically less complex because their strong resonance transitions enable efficient fluorescence detection and laser cooling. Standards based on $Ca^+$, $Sr^+$, and $Yb^+$ can be realized using commercially available low-power semiconductor laser sources. This will facilitate the development of compact systems, which are transportable and capable of an unattended long-term operation.

The upper levels of the reference transitions of the alkali-metal-like ions have a nonvanishing electric quadrupole moment. Even if the static electric stray field that arises at the trap center due to stray charges and surface potential inhomogeneities is nulled by compensation electrodes, the transition frequency is shifted by the interaction of the atomic quadrupole moment with the remaining field gradient. In order to eliminate the quadrupole shift, one must average over the transition frequencies measured for three mutually orthogonal orientations of the magnetic quantization field [10] or, alternatively, over the frequencies of several Zeeman components of the reference transition [5]. These measurement schemes have been successfully applied to absolute transition frequency measurements in $Hg^+$ [9], $Sr^+$ [5,6], and $Ca^+$ [4].

One expects that the magnitude and the temporal stability of the stray-field gradient are specific properties that depend on both the design of the trap and on its usage. These properties are of interest because they determine with which accuracy and speed the averaging must be carried out in order to eliminate the quadrupole shift with a low systematic uncertainty. However, it appears that only a few related observations have been reported up to now [5,11]. In this contribution, we present experimental results on the stability of the quadrupole shift in a single ion-frequency standard that is based on the $^2S_{1/2}-^2D_{3/2}$ transition of $^{171}Yb^+$ at 688 THz [7,12]. Using a differential measurement scheme, four quadrupole shift measurements with fractional uncertainties of less than $10^{-16}$ were conducted over a period of more than 70 days. During this period, also the absolute frequency of the reference transition was measured with averaging times of up to 90 h. The results of the quadrupole shift measurements were used to correct the measured optical frequencies. This allowed us to reduce the systematic uncertainty of the $^{171}Yb^+$ standard by a factor of 3 compared to previous measurements [13,14]. The total $1\sigma$ fractional uncertainty of the absolute frequency measurement reported here is $1.1\times10^{-15}$.

## II. OPTICAL EXCITATION AND MEASUREMENT SCHEME

A section of the energy-level scheme of $^{171}Yb^+$ is shown in Fig. 1. The reference transition of the 688 THz frequency standard is the $^2S_{1/2}(F=0)-^2D_{3/2}(F'=2)$ transition at 436 nm, which has a natural linewidth of 3.1 Hz. The $^2S_{1/2}-^2P_{1/2}$ resonance transition at 370 nm has a natural linewidth of 23 MHz. The quasicycling $F=1-F'=0$ hyperfine component of this transition is excited for laser cooling to a

 

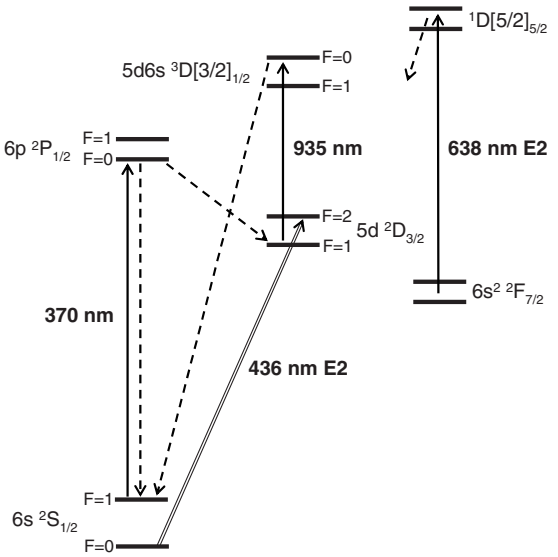


FIG. 1. Experimentally relevant part of the energy-level scheme of $^{171}Yb^+$ and employed optical-excitation scheme. Hyperfine-splitting frequencies are not drawn to scale. The dashed lines indicate major spontaneous decay paths.

Doppler limit temperature of 0.4 mK. This excitation also leads to a rapid branching spontaneous decay to the $F=1$ sublevel of the metastable $^2D_{3/2}$ state. For repumping, a transition at 935 nm to the $^3D[3/2]_{1/2}$ state is driven. If the 935 nm excitation is tuned to the $F=1-F'=0$ component of this transition and saturation broadening is avoided, the $^2D_{3/2}(F'=2)$ level is essentially decoupled from the laser cooling excitation cycle. This implies that the electron-shelving scheme can be used to detect individual transitions to this level by dark periods in the resonance fluorescence [15]. The dwell times in the $^2D_{3/2}(F'=2)$ level are much smaller than the natural lifetime of 53 ms if the 935 nm excitation is strongly saturated.

The lowest-lying excited state of $Yb^+$ is the extremely long-lived $^2F_{7/2}$ level. The excitation scheme shown in Fig. 1 provides no dipole-allowed spontaneous decay path to the $^2F_{7/2}$ level. We observe that the level is populated at a very low rate ($<1\ h^{-1}$) presumably as a result of level mixing induced by collisions and interactions with external fields. A transition at 638 nm is used to return the ion from the $^2F_{7/2}$ level to the laser cooling cycle [16].

In order to observe the resonance signal of the reference transition, a computer-controlled repetitive sequence of measurement cycles is run. Intervals of fluorescence detection, laser cooling, and state preparation are alternated with intervals where the cooling and the repumping lasers are blocked and a pulse of 436 nm probe light is applied. When the setup is operated as an optical frequency standard, the probe laser frequency is locked to the line center of the reference transition by a digital servo system. The error signal is generated by alternately stepping the excitation frequency up and down by equal amounts, so that the excitation occurs in the wings of the atomic resonance. After a few measurement cycles, the laser frequency is corrected in order to obtain equal excitation probabilities for both detunings. The employed second-order integrating servo algorithm minimizes servo errors that might be caused by laser frequency drift and measurement cycles with irregular state preparation of the ion. This locking scheme yields a fractional frequency stability (Allan deviation) of $\sigma_y(\tau)\approx 8\times 10^{-15}(\tau/\mathrm{s})^{-1/2}$ for $\tau\geq 30$ s if the $^{171}Yb^+$ reference transition is resolved with a Fourier-limited full half width of $\delta\nu\approx 30$ Hz. Numerical simulations indicate that the stability is essentially limited by quantum projection noise [17].

In order to determine frequency shifts of the reference transition that result from changes in operating conditions such as magnetic field orientation, we use a differential measurement scheme. The parameters of interest are periodically switched between two settings. The probe laser frequency corrections are determined independently for each setting through two alternately operating digital servos. The differences between the frequency corrections are recorded and averaged in order to obtain the frequency shift associated with the parameter variation. Similar dual or multiple optical frequency servo schemes have been adopted in a number of precision measurements on trapped ions [2,4,5,11,18,19].

## III. EXPERIMENTAL SETUP

A schematic of the experimental setup is shown in Fig. 2. The cooling radiation at 370 nm has a power of a few microwatts and is produced by a frequency-doubled 740 nm extended-cavity diode laser (ECDL). The diode current is modulated at a frequency of 14.5 GHz in order to generate a weak sideband in the 370 nm light that is resonant with the $F=0-F'=1$ component of the cooling transition, thereby compensating for optical pumping to the $^2S_{1/2}(F=0)$ state [15]. At the end of the cooling periods, the microwave modulation is switched off in order to prepare the ion in the $^2S_{1/2}(F=0)$ state. The frequency of the cooling laser is stabilized to the low-frequency wing of the $^2S_{1/2}(F=1)-{}^2P_{1/2}(F'=0)$ transition by a digital servo that keeps the fluorescence photon count rate during bright periods at a preset level. Transitions to the $^2F_{7/2}$ level and collisions with background gas atoms occasionally give rise to extended periods with a low or a vanishing fluorescence emission. If this condition persists for more than a few seconds, the cooling laser frequency is automatically scanned from a large red detuning toward line center in order to facilitate recooling of the ion.

Diode lasers are also used to generate the 935 and 638 nm repumping lights. During the initial $\approx 5$ ms of a cooling period, an acousto-optic modulator (AOM 1 in Fig. 2) reduces the power of the 935 nm light to approximately 20 $\mu$W. This allows us to determine whether the ion has been excited to the $^2D_{3/2}(F'=2)$ level by the preceding probe laser pulse (see above). For the rest of the cooling period, the 935 nm repumping power is in the range of 0.5 mW, so that both hyperfine sublevels of the $^2D_{3/2}$ level are efficiently depleted. The number of fluorescence photons that is registered while the 935 nm power is low is used in order to derive an error signal for the frequency stabilization of the 935 nm laser. The frequency of the 638 nm laser which depletes the $^2F_{7/2}$ level is swept at a frequency of $\approx 0.5$ Hz over the range of the hyperfine components of the 638 nm transition. The av-

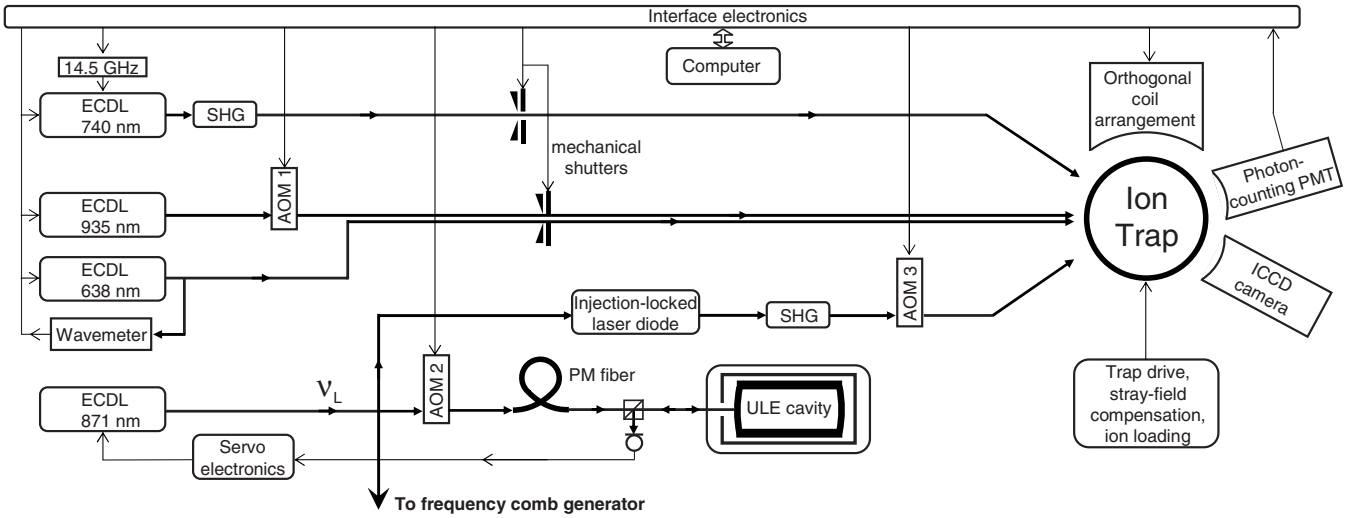


FIG. 2. Scheme of the experimental setup. ECDL: extended-cavity diode laser; AOM: acousto-optic modulator; SHG: second-harmonic generation; PM fiber: polarization-maintaining optical fiber; PMT: photomultiplier tube.

erage laser frequency is monitored by a wave meter for frequency stabilization. For a laser power in the range of 0.5 mW, dwell times in the $^2F_{7/2}$ level are typically shorter than 10 s.

Mechanical shutters are used for the cooling and the repumping lights in order to prevent ac Stark shifts of the reference transition during interaction with the probe laser light. The shutters consist of blackened sheet-metal strips attached to the axes of galvanometer motors. The shutters are inserted near intermediate focuses and are combined with diaphragms that suppress scattering light. For the 935 nm light, AOM 1 serves as an additional shutter. The cooling and the repumping beams are, respectively, focused to diameters of $\approx 50\ \mu$m and $\approx 100\ \mu$m in the trap.

The 436 nm probe light is produced by frequency doubling the output of an injection-locked laser diode. The injected light is the output of a 871 nm ECDL whose frequency is stabilized by an environmentally isolated high-finesse cavity made from ultralow expansion (ULE) glass (see Fig. 2). The linewidth of the free-running ECDL is in the range of 20 kHz. The Pound-Drever-Hall frequency locking scheme is realized by modulating the injection current of the ECDL at a frequency of $\approx 2$ MHz and by a phase-sensitive detection of the light reflected by the ULE cavity. In a vacuum of $\approx 3 \times 10^{-5}$ Pa the cavity is placed in a massive temperature-stabilized copper heat shield. The vacuum system and the coupling optics are mounted on a passive vibration isolation platform with vertical and horizontal resonance frequencies in the range of 0.5 Hz. The comparison with another similarly constructed laser system showed a combined fractional frequency instability (Allan deviation) of $\sigma_y(\tau) \approx 2 \times 10^{-15}$ for $0.1\ \mathrm{s} \leq \tau \leq 100\ \mathrm{s}$ [20]. The frequency drift rate of the cavity-stabilized probe laser varies in the range of −0.1 to 0.2 Hz/s over several hours.

As indicated in Fig. 2, the frequency of the 436 nm probe light is tuned by two acousto-optic modulators. AOM 3 alternately increases the second harmonic $2\nu_L$ of the probe laser frequency by $\Delta_3+\Delta_A$ or $\Delta_3-\Delta_A$ with $2\Delta_A \approx \delta\nu$. If no differential measurement is performed, the frequency $\Delta_3$ remains fixed and AOM 2 steers $2\nu_L+\Delta_3$ to the line center of the reference transition. Alternatively, in differential measurements where two probe laser frequency servos operate alternately (see above), one of the servos controls AOM 2 as just described. During the times when the other servo is active, $\Delta_3$ is corrected according to the difference between the servo outputs. Fundamental-frequency light at $\nu_L$ is forwarded to a fiber-laser based femtosecond frequency comb generator, which measures the optical frequency relative to a radiofrequency (rf) reference [21]. In the absolute frequency measurement described below, the rf reference is a 9.6 GHz standard frequency signal supplied by the cesium fountain clock CSF1 of PTB (Physikalisch-Technische Bundesanstalt) [22,23].

The employed ion trap is a cylindrically symmetric rf quadrupole trap with conical electrodes made from molybdenum [15]. The diameter of the ring electrode is 1.4 mm. Using a trap drive frequency of 15 MHz, under standard operating conditions the axial potential depth is $\approx 17$ eV and the axial and the radial secular oscillation frequencies are in the range of 1.4 and 0.7 MHz, respectively. In order to compensate the electric stray field at trap center in the axial direction, an adjustable dc voltage is applied between the trap end caps. Radial compensation voltages are applied to the Yb oven and to the electron-emitting filament that are used for ion loading. The stray field is compensated in three dimensions by minimizing the stray-field-induced displacement of the ion from the trap center when the potential depth is temporarily strongly reduced. After compensation, the residual offset from trap center is smaller than 100 nm, so that the kinetic energy of the micromotion is below $k \times 5$ mK, where $k$ is the Boltzmann constant [7,24].

The vacuum chamber of the trap is evacuated by an ion pump that provides a base pressure in the range of $10^{-7}$ Pa. At variance with earlier observations [25], we now find that at this pressure a trapped $Yb^+$ ion is usually lost during long periods ($\geq 5$ h) without laser cooling. The much longer storage time realized in the experiments described here was achieved by raising the background gas pressure in the trap

when no laser cooling is applied. This was done by operating the ion pump discontinuously with a low duty cycle of 300 s operation and 6000 s off period. The estimated background gas pressure at the end of the off periods is in the range of $10^{-5}-10^{-3}$ Pa. We attribute the extension of the storage time to the establishment of an equilibrium state where the heating of the ion by spurious electric field noise is balanced by the thermalization through collisions with background gas molecules. The formation of $YbH^+$ during this process is likely but it has been shown that $YbH^+$ is photodissociated if irradiated by 370 nm cooling laser light [26,27].

The magnetic field in the trap region is determined by an arrangement of coils that compensate the ambient static magnetic field and produce a quantization field of $\approx 4.5\ \mu$T. The resulting second-order Zeeman shift of the reference transition frequency is in the range of 1 Hz. The amplitude of ambient low-frequency alternating magnetic fields is below 50 nT. The field generated by one pair of coils is increased to $\approx 1$ mT during the laser cooling periods in order to reduce optical pumping between the magnetic sublevels of the $^2S_{1/2}(F=1)$ state. The orientation of the quantization field can be switched between three mutually orthogonal directions during measurements. The orthogonality of the field orientations was tested by measuring the splitting frequencies in the Zeeman pattern of the $^2S_{1/2}(F=0)-{}^2D_{3/2}(F'=2)$ reference transition for various combinations of coil currents. Deviations in the range of $1°-2°$ were found. The compensation of the ambient field was tested before and after each measurement run and the maximum error was kept below 100 nT. The compensation error results in an additional contribution of 2° to the orientation uncertainty of the magnetic field.

## IV. QUADRUPOLE SHIFT MEASUREMENTS

In good agreement with atomic-structure calculations [28,29], the electric quadrupole moment of the $^2D_{3/2}$ level of $Yb^+$ was determined as $\theta=9.32(48)\times 10^{-40}$ C m$^2$ [7]. The interaction between the quadrupole moment and an electric field gradient gives rise to a first-order quadrupole shift $\Delta\nu=h^{-1}A\theta g(\alpha,\beta)$, where $h$ is Planck's constant, $A$ denotes the magnitude of the electric field gradient, and $g(\alpha,\beta)$ is a geometrical factor determined by the symmetry of the gradient and its orientation relative to the quantization axis. The first-order quadrupole shifts that arise for three mutually orthogonal quantization axes add up to zero [10]. The same applies to the tensorial component of the quadratic Stark shift. For a rotationally symmetric gradient, $g(\alpha,\beta)=g(\beta)=3\cos^2\beta-1$, where $\beta$ denotes the angle between the symmetry axis and the quantization axis. Since in our case $\Delta\nu$ is much smaller than the Larmor frequency, the quantization axis is given by the orientation of the applied magnetic field and higher-order corrections to $\Delta\nu$ are negligible.

The field gradient produced by applying a dc voltage $U$ to the ring electrode of the trap has the magnitude $A=U/d_0^2$, where $d_0=1.06$ mm is determined by the size and the electrode design of the employed trap. Using a differential measurement scheme as described above, the angles

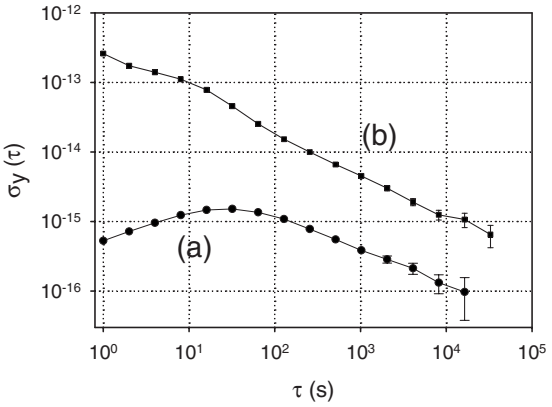


FIG. 3. Allan deviation $\sigma_y(\tau)$ as a function of averaging time $\tau$ of (a) a differential measurement of the transition frequency difference $\Delta\nu_{23}$ that arises if the quantization field is varied between two orthogonal orientations (see text) and (b) of an absolute frequency measurement of 90 h duration. The frequency fluctuations are normalized to the frequency of the $Yb^+$ standard (688 THz).

$\beta_i$ $(i=1,2,3)$ between the trap axis and the preset magnetic field orientations were determined by measuring the quadrupole shifts that result if $U$ is increased from 0 to 10 V. This differential measurement offers the advantage that it is not sensitive to the stray-field-induced quadrupole shift and to the Stark shift because these perturbations are not expected to vary significantly if $U$ is varied in the range indicated. For the magnetic field orientations $i=1$, 2, and 3, the respective measured quadrupole shifts are −6.6(6), −0.8(6), and 7.3(6) Hz. Here, the numbers in parentheses denote $1\sigma$ statistical uncertainties. As expected for orthogonal magnetic field orientations, the sum of the shifts does not significantly deviate from zero. The inferred angles between the magnetic field orientations and the trap axis are $\beta_1=66.6(1.3)°$, $\beta_2=56.0(1.0)°$, and $\beta_3=43.4(9)°$.

If no field gradient is applied externally $(U=0)$ and the transition frequency is measured for three orthogonal orientations of the quantization field, the shift of the transition frequency caused by the stray-field gradient (quadrupole shift) and the tensorial Stark shift can be inferred from the observed frequency differences. Specifically, denoting the shifted transition frequency with $\nu_i=\nu+\delta_i$ $(i=1,2,3)$, where $\nu$ is the unshifted frequency and $\delta_i$ is the orientation-dependent shift, we determine the frequency differences $\Delta\nu_{13}=\nu_1-\nu_3$ and $\Delta\nu_{23}=\nu_2-\nu_3$ that arise if the magnetic field orientation is varied between $i=1$ and $i=3$ and between $i=2$ and $i=3$, respectively. Since the magnetic field orientations are very close to orthogonal, we assume that $\delta_1+\delta_2+\delta_3=0$, so that the orientation-dependent shifts are given by $\delta_3=-(\Delta\nu_{13}+\Delta\nu_{23})/3$, $\delta_2=(2\Delta\nu_{23}-\Delta\nu_{13})/3$, and $\delta_1=(2\Delta\nu_{13}-\Delta\nu_{23})/3$.

We measured the frequency differences $\Delta\nu_{13}$ and $\Delta\nu_{23}$ immediately before loading the trap with a new ion and three more times during the subsequent storage period of 74 days. In these measurements, the reference transition was resolved with a Fourier-limited linewidth $\delta\nu\approx 30$ Hz in a measurement cycle time of 73 ms; the magnetic field orientation was alternated every 4 cycles. The averaging times were typically in the range of 15 h. Figure 3(a) shows a typical Allan de-

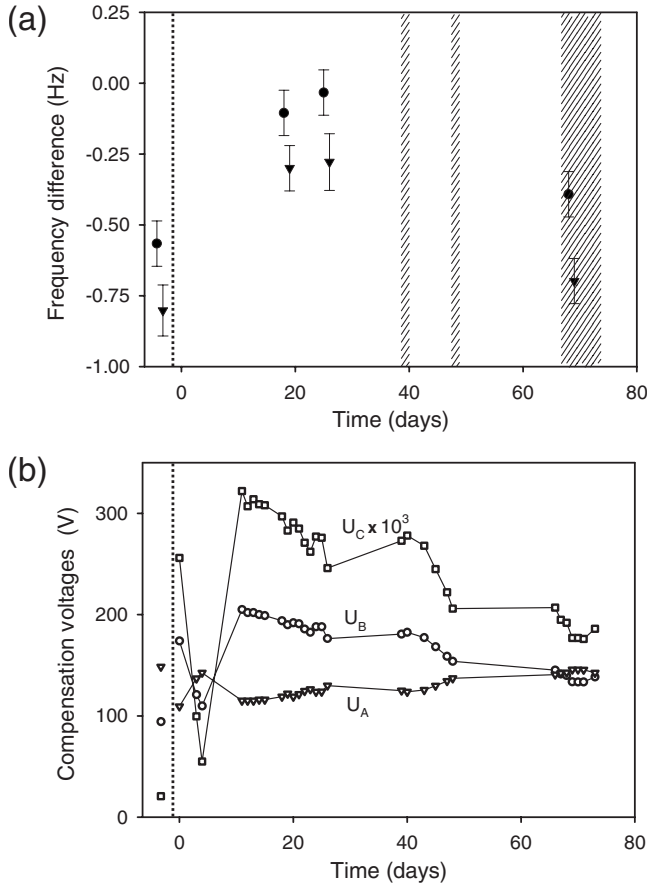


FIG. 4. Temporal variation of (a) the observed frequency differences $\Delta\nu_{13}$ (dots) and $\Delta\nu_{23}$ (triangles) and of (b) the stray-field compensation voltages applied between the trap end caps ($U_C$) and to the Yb oven ($U_B$) and the electron source ($U_A$). The vertical dotted line denotes the time when a new ion was loaded. The data points to the left of the dotted vertical line correspond to measurements done immediately before ion loading. The hatched areas in (a) denote the periods when absolute frequency measurements were carried out. For further details, see text.

viation of recorded frequency difference data. The averaging time of $\tau \approx 30$ s when $\sigma_y(\tau)$ is maximal is determined by the approximately equal time constants of the alternately operating servo systems. For $\tau > 100$ s, the Allan deviation indicates a white-noise characteristic without significant drift. The observed instability of $\sigma_y(\tau) \approx 1.1 \times 10^{-14}(\tau/\mathrm{s})^{-1/2}$ appears to be determined by quantum projection noise. The results of the frequency difference measurements are summarized in Fig. 4(a). The displayed data include a second-order Zeeman shift correction of 0.14 Hz in order to compensate for the slightly larger magnetic field applied in the $i=3$ orientation. The measurement uncertainty is dominated by the uncertainty associated with the compensation of the ambient magnetic field (see above). Assuming uncorrelated variations of the three spatial components of the magnetic field, the uncertainty of $\Delta\nu_{13}$ and $\Delta\nu_{23}$ due to variations in the second-order Zeeman shift is 0.07 Hz. The statistical measurement uncertainty is typically smaller than 0.04 Hz.

The data shown in Fig. 4(a) demonstrate large relative variations in $\Delta\nu_{13}$ and $\Delta\nu_{23}$ during the observation period. We attribute these variations to changes in the strength and orientation of the electric stray-field gradient. Previous comparisons between two $^{171}Yb^+$ standards which were carried out under similar experimental conditions with traps of the same design indicated no Stark shifts of comparable magnitude that might contribute to $\Delta\nu_{13}$ and $\Delta\nu_{23}$ [7,24]. The largest magnetic-field-orientation-dependent frequency shift that is inferred from the present measurements [leftmost data points in Fig. 4(a)] is $\delta_3 = 0.46(4)$ Hz.

It is well known that the static electric stray field in ion traps can be altered strongly if neutral atoms are evaporated and ionized by electron impact. Much smaller changes are observed if ions are loaded by photoionization [30]. Figure 4(b) shows the temporal variation of the compensation voltages during the measurements. We expect that in our trap setup the radial stray-field compensation voltages contribute significantly to the field gradient at the trap center, so that the temporal variations of compensation voltages and stray-field gradient should be partly correlated. The data shown in Fig. 4(b) indicate that the compensation voltages vary rapidly during the days after ion loading. In the longer term, the compensation voltages as well as $\Delta\nu_{13}$ and $\Delta\nu_{23}$ tend toward their initial values. The compensation voltages, in particular $U_C$ which is applied between the trap end caps, show relatively small variations during the periods when no measurements were done and no laser light passed through the trap. This seems to indicate that the illumination of the trap electrodes or of nearby components by laser stray light contributed to the observed long-term variation in the electric stray field.

## V. MEASUREMENT OF THE ABSOLUTE TRANSITION FREQUENCY

In previous measurements of the frequency of the $^{171}Yb^+$ $^2S_{1/2}(F=0)-{}^2D_{3/2}(F'=2)$ transition, the systematic uncertainty was dominated by a 1 Hz contribution from the stray-field-induced quadrupole shift [13,14]. This uncertainty estimate was based on comparisons between two ion traps [7,24]. The absolute frequency was measured again in the course of the investigations described above. The corresponding measurement periods are indicated in Fig. 4(a). The measurement of $\Delta\nu_{13}$ and $\Delta\nu_{23}$ allows one to significantly reduce the systematic uncertainty of the $^{171}Yb^+$ standard even though only one of the absolute frequency measurement runs was carried out simultaneously with a measurement of $\Delta\nu_{13}$ and $\Delta\nu_{23}$.

During the time of the measurements, the cesium fountain reference CSF1 was operated under conditions where its estimated systematic fractional frequency uncertainty is $0.9 \times 10^{-15}$. The statistical uncertainty of the optical frequency measurement is essentially determined by the instability of the fountain. As indicated in Fig. 3(b), the instability averages down as $\sigma_y(\tau) \approx 1 \times 10^{-13}(\tau/\mathrm{s})^{-1/2}$. Averaging times in the range of 25 to 90 h were used in order to obtain low statistical uncertainties. The results of the absolute frequency measurements are summarized in Table I. The listed results are corrected for known perturbations (see below) apart from the quadratic Stark shift of the $Yb^+$ transition frequency due

TABLE I. Results[a] and uncertainty contributions of the absolute frequency measurements conducted in 2008. All uncertainty data are scaled to the frequency of the $^{171}Yb^+$ standard (688 THz). The results are not corrected with respect to the blackbody shift (see text). The measured frequencies are $\nu = 688\ 358\ 979\ 309\ 000\ \text{Hz} + C\ \text{Hz}$.

| Starting date of measurement | Result $C$ (Hz) | Statistical uncertainty (Hz) | Systematic uncertainty, CSF1 (Hz) | Systematic uncertainty, $^{171}Yb^+$ (Hz) |
|---|---|---|---|---|
| 2008-8-6 | 306.59 | 0.50 | 0.62 | 0.31 |
| 2008-8-13 | 306.76 | 0.45 | 0.62 | 0.31 |
| 2008-9-3 | 306.53 | 0.30 | 0.62 | 0.31 |

[a]Weighted mean and total uncertainty: $\nu[^{171}Yb^+, {}^2S_{1/2}(F=0) - {}^2D_{3/2}(F'=2)] = 688\ 358\ 979\ 309\ 306.62(73)\ \text{Hz}$

to the ambient blackbody radiation. The trap was operated at room temperature ($T=300$ K). For this case, a blackbody shift of $-0.35(7)$ Hz is calculated on the basis of measurements of the static atomic polarizability [31].

The individual measurement results contribute to the weighted mean noted in Table I with weights proportional to $[u_A^2(i) + u_B^2(\text{Cs}) + u_B^2(\text{Yb}^+)]^{-1}$. Here, $u_A(i)$ $(i=1,2,3)$ denotes the statistical uncertainties of the results and $u_B(\text{Cs})$ and $u_B(\text{Yb}^+)$, respectively, denote the systematic uncertainties of CSF1 and of the $^{171}Yb^+$ standard as given in Table I. The total uncertainty is calculated as $[u_A^2 + u_B^2(\text{Cs}) + u_B^2(\text{Yb}^+)]^{1/2}$ with $u_A = \{\Sigma_i [u_A(i)]^{-2}\}^{-1/2}$. The inferred uncertainty of the $^{171}Yb^+$ standard of 0.31 Hz corresponds to a fractional uncertainty of $5 \times 10^{-16}$ and is a factor of 3 smaller than that of the measurements conducted in 2005–2006 [13,14]. The difference between the present and the previous absolute frequency results is 1.1 Hz, which is within the estimated total systematic uncertainty of the previous measurement.

The leading contributions to the systematic uncertainty of the $^{171}Yb^+$ standard are listed in Table II. For two of the three absolute frequency measurement runs, the quadrupole and tensorial Stark shift correction was determined by linear interpolation between the results of the preceding and the subsequent measurements of $\Delta\nu_{13}$ and $\Delta\nu_{23}$. In order to take into account the lack of information on the actual temporal variation of $\Delta\nu_{13}$ and $\Delta\nu_{23}$, we assume an uncertainty of the calculated corrections of 0.2 Hz, which is comparable to their maximum variation during the measurement period. Scalar ac Stark shifts potentially caused by laser stray light and environmental blackbody radiation sources are taken into account with an uncertainty contribution of 0.2 Hz. This estimate is based on the results of comparisons between two $^{171}Yb^+$ standards [7,24]. The servo error contribution of 0.1 Hz takes into account deviations of the average probe laser frequency from the atomic line center frequency that can be caused by laser frequency drift and asymmetric spurious components of the probe light spectrum. Other frequency shifting effects such as the Doppler and the Stark shifts caused by the residual ion motion and second-order Zeeman shifts due to alternating magnetic fields are not listed in Table I because the estimated frequency shifts and uncertainty contributions are smaller than 0.01 Hz.

## VI. SUMMARY

We have carried out an investigation of frequency shifts in a $^{171}Yb^+$ single-ion optical frequency standard that occur due to the interaction of the atomic electric quadrupole moment with the gradient of the electrostatic stray field in the trap. The observed maximum fractional quadrupole shift is $0.67(6) \times 10^{-15}$. We find that the short-term instability of the shift is below the quantum projection noise limit for averaging times of up to 20 h, but significant variations in the $10^{-16}$ range occur during the observation period of 74 days. The relative variations in the quadrupole shift are somewhat larger than the relative variations in the voltages that are applied to compensate the electric stray field at trap center. Our observations confirm that the quadrupole shift in fact can be eliminated with a high accuracy through measurement schemes that rely on averaging over the shifts that appear in orthogonal magnetic field orientations or in different Zeeman components of the reference transition [5,10]. However, the observed long-term variation of the shift suggests that averaging over intervals of more than a few hours could entail significant systematic errors.

TABLE II. Applied frequency corrections and leading contributions ($\geq 0.01$ Hz) to the systematic uncertainty of the 688-THz $^{171}Yb^+$ single-ion optical frequency standard.

| Physical Effect | Correction (Hz) | Uncertainty (Hz) |
|---|---|---|
| Second-order Zeeman shift | −1.13 | 0.05 |
| Quadrupole shift and tensorial quadratic Stark shift | −0.36 to −0.19 | 0.2 |
| Scalar ac Stark shift | 0 | 0.2 |
| Servo error | 0 | 0.1 |
| Total | −1.43 to −1.26 | 0.31 |

During the period of the quadrupole shift measurements, we also performed a measurement of the absolute frequency of the $^2S_{1/2}(F=0)-{}^2D_{3/2}(F'=2)$ transition of $^{171}Yb^+$. The determination of the quadrupole shift allowed us to significantly reduce the systematic uncertainty of the 688-THz $^{171}Yb^+$ standard relative to previous measurements. The frequency measured at 300 K temperature is $\nu = 688\,358\,979\,309\,306.62(73)$ Hz. The estimated total $1\sigma$ uncertainty of 0.73 Hz corresponds to a fractional uncertainty of $1.1\times10^{-15}$, which is determined mainly by the systematic uncertainty of the employed cesium fountain reference.

## ACKNOWLEDGMENT

This work was partly supported by Deutsche Forschungsgemeinschaft in SFB 407.

[1] A. D. Ludlow *et al.*, Science **319**, 1805 (2008).
[2] T. Rosenband *et al.*, Science **319**, 1808 (2008).
[3] Th. Becker, J. v. Zanthier, A. Yu. Nevsky, Ch. Schwedes, M. N. Skvortsov, H. Walther, and E. Peik, Phys. Rev. A **63**, 051802(R) (2001).
[4] M. Chwalla *et al.*, Phys. Rev. Lett. **102**, 023002 (2009).
[5] P. Dubé, A. A. Madej, J. E. Bernard, L. Marmet, J. S. Boulanger, and S. Cundy, Phys. Rev. Lett. **95**, 033001 (2005).
[6] H. S. Margolis, G. P. Barwood, G. Huang, H. A. Klein, S. N. Lea, K. Szymaniek, and P. Gill, Science **306**, 1355 (2004).
[7] T. Schneider, E. Peik, and Chr. Tamm, Phys. Rev. Lett. **94**, 230801 (2005).
[8] K. Hosaka, S. A. Webster, A. Stannard, B. R. Walton, H. S. Margolis, and P. Gill, Phys. Rev. A **79**, 033403 (2009).
[9] W. H. Oskay *et al.*, Phys. Rev. Lett. **97**, 020801 (2006).
[10] W. M. Itano, J. Res. Natl. Inst. Stand. Technol. **105**, 829 (2000).
[11] W. H. Oskay, W. M. Itano, and J. C. Bergquist, Phys. Rev. Lett. **94**, 163001 (2005).
[12] E. Peik, B. Lipphardt, H. Schnatz, T. Schneider, Chr. Tamm, and S. G. Karshenboim, Phys. Rev. Lett. **93**, 170801 (2004).
[13] Chr. Tamm, B. Lipphardt, H. Schnatz, R. Wynands, S. Weyers, T. Schneider, and E. Peik, IEEE Trans. Instrum. Meas. **56**, 601 (2007).
[14] E. Peik, B. Lipphardt, H. Schnatz, Chr. Tamm, S. Weyers, and R. Wynands, in *Proceedings of the 11th Marcel Grossmann Meeting on General Relativity*, edited by H. Kleinert, R. T. Jantzen, and R. Ruffini (World Scientific, Singapore, 2007); e-print arXiv:physics/0611088v1.
[15] Chr. Tamm, D. Engelke, and V. Bühner, Phys. Rev. A **61**, 053405 (2000).
[16] P. Gill, H. A. Klein, A. P. Levick, M. Roberts, W. R. C. Rowley, and P. Taylor, Phys. Rev. A **52**, R909 (1995).
[17] E. Peik, T. Schneider, and Chr. Tamm, J. Phys. B **39**, 145 (2006).
[18] G. P. Barwood, H. S. Margolis, G. Huang, P. Gill, and H. A. Klein, Phys. Rev. Lett. **93**, 133001 (2004).
[19] J. E. Bernard, L. Marmet, and A. A. Madej, Opt. Commun. **150**, 170 (1998).
[20] B. Lipphardt, G. Grosche, U. Sterr, Chr. Tamm, S. Weyers, and H. Schnatz, IEEE Trans. Instrum. Meas. **58**, 1258 (2009).
[21] P. Kubina *et al.*, Opt. Express **13**, 904 (2005).
[22] S. Weyers, U. Hübner, R. Schröder, Chr. Tamm, and A. Bauch, Metrologia **38**, 343 (2001).
[23] S. Weyers, A. Bauch, R. Schröder, and Chr. Tamm, in *Proceedings of the 6th Symposium Frequency Standards and Metrology*, edited by P. Gill (World Scientific, Singapore, 2002), p. 64.
[24] T. Schneider, Ph.D. thesis, Hannover University, Hannover, Germany, 2005.
[25] Ch. Tamm, T. Schneider, and E. Peik, in *Laser Spectroscopy XVI*, edited by P. Hannaford, A. Sidorov, H. Bachor, and K. Baldwin (World Scientific, Singapore, 2004), p. 40.
[26] A. Bauch, D. Schnier, and Chr. Tamm, J. Mod. Opt. **39**, 389 (1992).
[27] K. Sugiyama and J. Yoda, Phys. Rev. A **55**, R10 (1997).
[28] W. M. Itano, Phys. Rev. A **73**, 022510 (2006).
[29] K. V. P. Latha, C. Sur, R. K. Chaudhuri, B. P. Das, and D. Mukherjee, Phys. Rev. A **76**, 062508 (2007).
[30] S. Gulde, D. Rotter, P. Barton, F. Schmidt-Kaler, R. Blatt, and W. Hogervorst, Appl. Phys. B: Lasers Opt. **73**, 861 (2001).
[31] S. N. Lea, S. A. Webster, and G. P. Barwood, *Proceedings of the 20th European Frequency and Time Forum, Braunschweig, 2006* (PTB, Braunschweig, Germany, 2006, p. 302.